NANO LETTERS

Letter

pubs.acs.org/NanoLett

Reversibility of Noble Metal-Catalyzed Aprotic Li-O_2 Batteries

Shunchao Ma,[†,‡] Yang Wu,[*,§] Jiawei Wang,[†] Yelong Zhang,[†,‡] Yantao Zhang,[†,‡] Xinxiu Yan,[†] Yang Wei,[§] Peng Liu,[§] Jiaping Wang,[§] Kaili Jiang,[§] Shoushan Fan,[§] Ye Xu,[∥] and Zhangquan Peng[*,†]

[†]State Key Laboratory of Electroanalytical Chemistry, Changchun Institute of Applied Chemistry, Chinese Academy of Sciences, Changchun 130022, P. R. China

[‡]University of Chinese Academy of Sciences, Beijing 100039, P. R. China

[§]Department of Physics and Tsinghua-Foxconn Nanotechnology Research Center, Tsinghua University, Beijing 100084, P. R. China

[∥]Department of Chemical Engineering, Louisiana State University, Baton Rouge, Louisiana 70803, United States

Supporting Information

ABSTRACT: The aprotic Li-O_2 battery has attracted a great deal of interest because, theoretically, it can store far more energy than today's batteries. Toward unlocking the energy capabilities of this neotype energy storage system, noble metal-catalyzed high surface area carbon materials have been widely used as the O_2 cathodes, and some of them exhibit excellent electrochemical performances in terms of round-trip efficiency and cycle life. However, whether these outstanding electrochemical performances are backed by the reversible formation/decomposition of Li_2O_2, i.e., the desired Li-O_2 electrochemistry, remains unclear due to a lack of quantitative assays for the Li-O_2 cells. Here, noble metal (Ru and Pd)-catalyzed carbon nanotube (CNT) fabrics, prepared by magnetron sputtering, have been used as the O_2 cathode in aprotic Li-O_2 batteries. The catalyzed Li-O_2 cells exhibited considerably high round-trip efficiency and prolonged cycle life, which could match or even surpass some of the best literature results. However, a combined analysis using differential electrochemical mass spectrometry and Fourier transform infrared spectroscopy, revealed that these catalyzed Li-O_2 cells (particularly those based on Pd-CNT cathodes) did not work according to the desired Li-O_2 electrochemistry. Instead the presence of noble metal catalysts impaired the cells' reversibility, as evidenced by the decreased O_2 recovery efficiency (the ratio of the amount of O_2 evolved during recharge/that consumed in the preceding discharge) coupled with increased CO_2 evolution during charging. The results reported here provide new insights into the O_2 electrochemistry in the aprotic Li-O_2 batteries containing noble metal catalysts and exemplified the importance of the quantitative assays for the Li-O_2 reactions in the course of pursuing truly rechargeable Li-O_2 batteries.

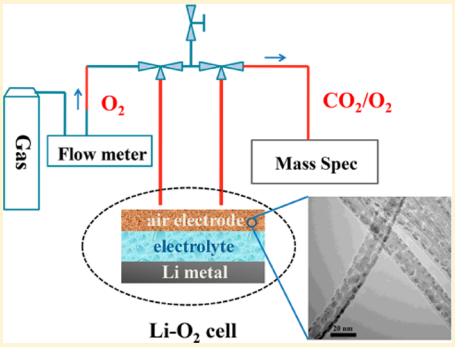

KEYWORDS: *Aprotic Li-O_2 battery, O_2 reduction/evolution reaction, differential electrochemical mass spectrometry, noble metal catalyst, reversibility*

The aprotic Li-O_2 battery has been considered as a promising candidate for next generation energy storage systems, on account of its potential to deliver 3−5 times more energy than today's Li-ion batteries.[1−5] Operation of the aprotic Li-O_2 battery relies critically on the reversible reactions of Li and O_2 ($2Li + O_2 \leftrightarrow Li_2O_2$, E^0 = 2.96 V vs Li/Li^+). Although the chemistry underlying the ideal Li-O_2 batteries seems straightforward, the practical application of this new type of energy storage system has been impeded by a number of technical challenges, such as low round-trip efficiency, degraded capacity and cyclability, and limited stability of the battery components.[6,7] These challenges are strongly associated with the kinetics of the growth/decomposition of the insulating and insoluble Li_2O_2 during the discharge/recharge cycle[7] and the possible parasitic reactions involving the degradation of the cathode materials and electrolytes.[8] To improve the electrochemical performances of the aprotic Li-O_2 batteries, considerable research efforts have been devoted to the search for more stable electrolytes that can resist the attack of the O_2 reduction intermediates and products.[9−13] Meanwhile, sizable endeavors have been focused on the fabrication of nanostructured and catalyzed O_2 cathodes, and numerous combinations of catalysts and conductive matrixes have been studied.[9,14−45] For instance, noble metals,[9,14−18] transition-metal oxides,[19−26] and soluble redox mediators[27−29] have been tried as the catalysts in the aprotic Li-O_2 batteries. Both carbon (graphene and carbon nanotube [CNT])[30−36] and noncarbon materials (TiC, indium tin oxide (ITO), Sb-doped SnO_2, and $TiSi_2$)[37−40] have been employed as the O_2 cathode host materials with some of the latter exhibiting better stability than the former. Among all these efforts, Li-O_2 batteries based on noble metal-catalyzed carbon materials frequently demonstrate remarkable performances in terms of energy efficiency and

Received: September 1, 2015
Revised: November 2, 2015
Published: November 4, 2015

DOI: 10.1021/acs.nanolett.5b03510
Nano Lett. 2015, 15, 8084−8090

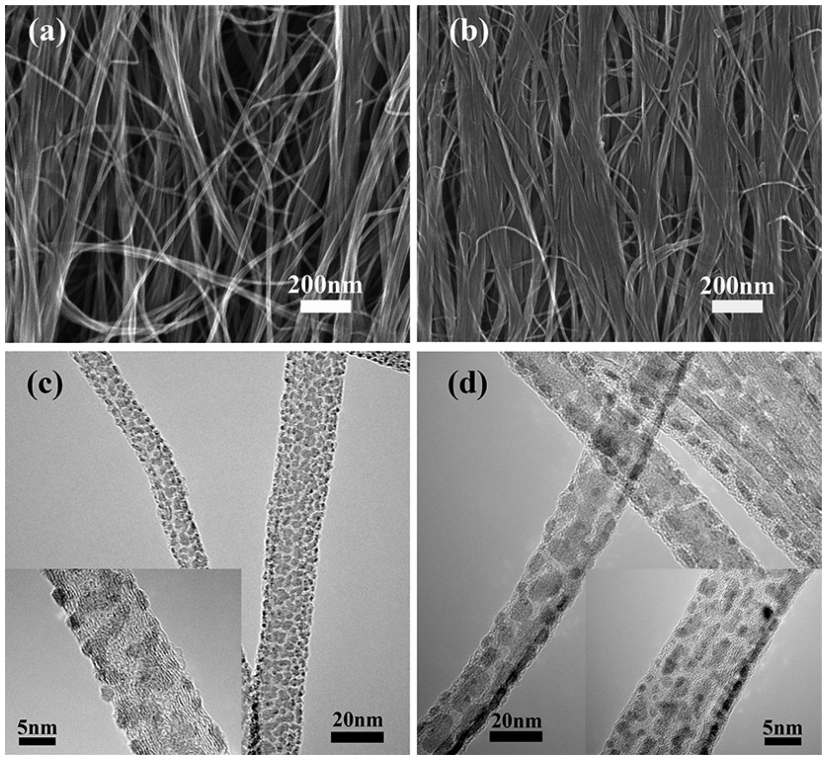

Figure 1. SEM images of (a) Ru-CNT and (b) Pd-CNT fabric electrodes, and TEM images of (c) Ru-CNT and (d) Pd-CNT fabric electrodes. Insets in (c) and (d) are the TEM images with higher magnifications.

cycle life.[41−45] For instance, Zeng et al. reported that Ru nanoparticles supported on multielement codoped graphene can greatly improve Li-O_2 cell's capacity and cycle stability (>300 cycles).[44] Shen et al. demonstrated that Pd-decorated CNT sponge cathode not only improved the catalytic activity but also delivered excellent capacity and cycle performance in ambient air.[45]

It is worth noting that most of these studies did not conclusively provide experimental evidence that the reversible formation/decomposition of Li_2O_2, i.e., the desired Li-O_2 reactions, underlies the operation of these noble metal-catalyzed Li-O_2 cells. Instead only qualitative studies, including powder X-ray diffraction (XRD), scanning electron microscope (SEM), transmission electron microscope (TEM), X-ray photoelectron spectroscopy (XPS), etc., have been conducted to follow the O_2 reactions in the cathodes, which, as pointed out recently by McCloskey et al.,[8] are inadequate to fully address the Li-O_2 electrochemistry.

For the purpose of dynamical and quantitative study of the gaseous electrode reactions, differential electrochemical mass spectrometry (DEMS) has been proved to be an indispensible *in situ* characterization technique, which has been successfully employed in real time studies of the electrochemical reactions in fuel cells,[46−48] Li-ion[49−51] and Li-O_2 batteries.[9,12,27,52−55] As for the O_2 reactions in the aprotic Li-O_2 batteries, DEMS has the ability to quantify the amount of the O_2 that is consumed during discharge and evolves during recharge. Moreover, it can simultaneously monitor other gaseous products from possible parasitic reactions, providing invaluable information for the understanding of the fundamental electrochemistry, e.g., reversibility, of the aprotic Li-O_2 batteries. For ideally rechargeable (or reversible) aprotic Li-O_2 batteries without any parasitic reactions, the discharge product of Li_2O_2 would be formed/decomposed via a $2e^-/O_2$ process, and the amount of the O_2 consumed during discharge would be equal to that evolved during recharge. For those noble metal-catalyzed Li-O_2 batteries, it is crucial to know whether they operate with desired reversibility according to the ideal Li-O_2 electrochemistry, which is an essential prerequisite for the truly rechargeable Li-O_2 batteries.

In this Letter, noble metal (Ru and Pd)-catalyzed carbon nanotube (CNT) fabrics have been prepared by magnetron sputtering and used directly as the O_2 cathode in aprotic Li-O_2 batteries. The Ru/Pd-CNT electrodes with unique nanostructures can facilitate the transport of reactants and provide excellent catalytic activity toward O_2 reactions. As expected, the catalyzed Li-O_2 batteries demonstrated outstanding electrochemical performances including high round-trip efficiency and long cycle life (100 cycles), which could match or even surpass some of the best literature results. However, DEMS studies revealed that these noble metal-catalyzed Li-O_2 batteries (particularly Pd-CNT) did not work according to the desired Li-O_2 reactions, as evidenced by the decreased O_2 recovery efficiency (the ratio of the amount of O_2 evolved during recharge/that consumed in the preceding discharge) coupled with increased CO_2 evolution during charging, suggesting a reversibility even poorer than their counterpart using pristine CNT cathodes. The results reported here provide new insights into the O_2 electrochemistry of the aprotic Li-O_2 batteries containing noble metal catalysts and exemplify the importance of quantitative assays for the Li-O_2 electrochemistry in the course of pursuing truly rechargeable Li-O_2 batteries.

Results and Discussion. Noble metal (Ru and Pd)-catalyzed CNT fabrics were prepared by a magnetron sputtering method, in which the spinnable superaligned CNT yarns, reeled from superaligned CNT arrays on a Si wafer, were drawn above a vertically placed sputtering gun (Supporting Information Figure S1). Bulk Ru and Pd metals with high

DOI: 10.1021/acs.nanolett.5b03510
Nano Lett. 2015, 15, 8084−8090

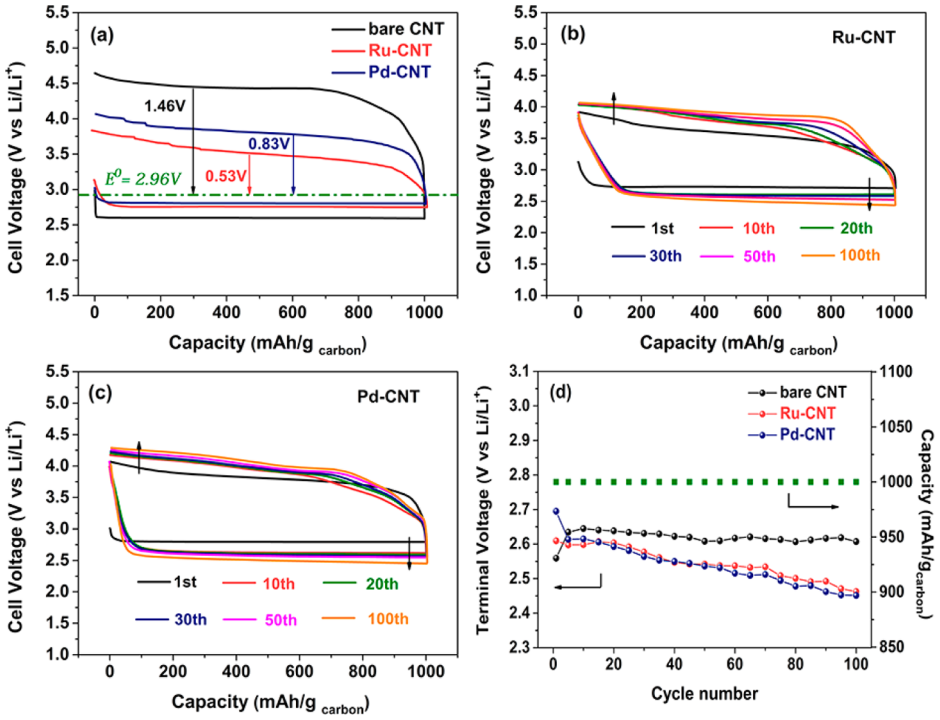

Figure 2. (a) The first cycle of the pristine CNT (black), Ru-CNT (red), and Pd-CNT (blue) cathodes operated with a fixed capacity of 1000 mA/g_{carbon}. Multiple cycles from 1 to 100 of the catalyzed Li-O_2 cells based on (b) Ru-CNT and (c) Pd-CNT cathodes, and (d) the terminal discharge voltage as a function of cycle number at a fixed capacity of 1000 mAh/g_{carbon}. A current density of 500 mA/g_{carbon} was used for the above Li-O_2 cells.

purity (99.95%) were used as the targets. The growth of superaligned CNT arrays on Si was briefly described in the Supporting Information, and more technical details can be found in our previous reports.[56−58] Such a fabrication process resulted in a porous electrode structure (Figure 1a,b) that was expected to be easily wetted by organic electrolytes when used as the cathode for the aprotic Li-O_2 batteries. Sputtered Ru and Pd nanoparticles with an average size of ca. 3−4 nm were coated on the CNT sidewalls in a conformal manner, as shown in a TEM study (Figure1c,d). The chemical composition and phase analysis of the noble metal-catalyzed CNT cathodes were provided by energy dispersive X-ray spectroscopy (EDX) (Supporting Information Figure S2a,b) and XRD (Supporting Information Figure S2c,d) analyses, which confirmed the exclusion of O_2 contamination during the sample preparation process. The mass loadings of the noble metal nanoparticles on the CNT electrodes were determined by thermogravimetric analysis (TGA, 76% for Ru-CNT and 83.3% for Pd-CNT, Supporting Information Figure S3a,b). Based on the above structural and compositional analyses, it was concluded that the nanostructured Ru/Pd-CNT electrodes would be able to facilitate the transport of both dissolved O_2 and Li^+ and maximize the utilization of Ru and Pd nanoparticles for their catalytic effects.

The electrochemical performances of Ru-CNT and Pd-CNT cathodes were studied in a Swagelok-type Li-O_2 cell using 0.1 M LiTFSI in tetraethylene glycol dimethyl ether as the electrolyte. A pristine CNT fabric electrode was also investigated as a control experiment. The load curves of the pristine and catalyzed CNT electrodes, which were cycled with a fixed capacity of 1000 mAh/g_{carbon} at a current density of 500 mA/g_{carbon}, are shown in Figure 2a−c. For the first cycle (Figure 2a), a discharge plateau at 2.8 V for Pd-CNT and 2.75 V for Ru-CNT was obtained, compared to 2.6 V for the pristine CNT, indicating modest catalytic performances toward the discharge reaction (O_2 reduction reaction, ORR) on the catalyzed CNT cathodes, consistent with previous findings.[7,59] However, both the Ru-CNT and Pd-CNT electrodes greatly facilitated the charging reaction (O_2 evolution reaction, OER) by reducing the charging overpotentials by ∼930 and ∼630 mV, respectively, with respect to that of the pristine CNT cathode at the same current density. These results may suggest a better electrocatalytic activity of Ru-CNT and Pd-CNT electrodes toward both ORR and OER as claimed in recent reports.[41,43−45] The cyclability of the catalyzed Li-O_2 cells was also measured, and the results are shown in Figure 2b,c. It was observed that the discharge plateaus of Ru/Pd-CNT cathodes decreased gradually as a function of cycle number, and meanwhile the recharge plateaus increased. In contrast, the discharge and recharge potential plateaus of the pristine CNT electrode remained almost unvaried in the cycle numbers of 1−100, despite relatively high overpotentials involved during charging (Supporting Information Figure S4). A comparison of the cycle stability of the pristine and the catalyzed Li-O_2 cells, by plotting the terminal discharge voltage as a function of cycle number, is shown in Figure 2d. The gradual decrease in the terminal discharge voltage of the catalyzed Li-O_2 cells suggested that the presence of nanosized Ru/Pd catalysts probably degraded the reaction reversibility, despite the fact that the overpotentials for recharge were initially reduced, compared to the pristine CNT electrode.

To build rechargeable electrochemical energy storage devices, the reversibility of the electrochemical reactions on which operation of the devices depends is an essential prerequisite. Evaluation of the reversibility of a full discharge/recharge cycle was performed by monitoring the O_2 consumption/evolution rate and the coupled charge passed using a quantitative DEMS. In an ideally reversible electro-

DOI: 10.1021/acs.nanolett.5b03510
Nano Lett. 2015, 15, 8084−8090

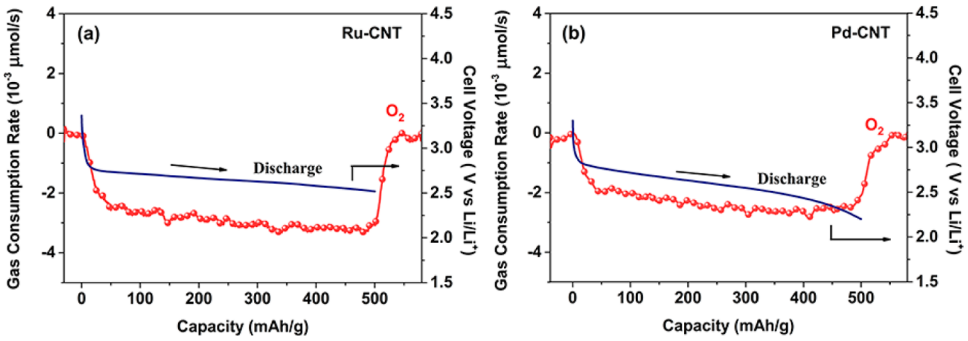

Figure 3. DEMS results of O_2 gas consumption during discharge of Li-O_2 cells based on (a) Ru-CNT and (b) Pd-CNT cathodes. The Li-O_2 cells were discharged with a fixed capacity of 500 mAh/g at a constant current of 0.6 mA.

Table 1. Gases Consumed and Evolved in a Full Cycle of Li-O_2 Cells Quantified with DEMS[a]

	charge passed		O_2 quantity		(e^-/O_2)		CO_2 quantity		
cell cathode	D(a)	R(a)	C(a)	E(a)	D	R	C(a)	E(a)	OER/ORR
CNT	18.701	18.701	9.274	6.070	2.02	3.08	—	0.621	0.654
Ru-CNT	18.640	18.640	8.960	5.931	2.08	3.14	—	1.253	0.662
Pd-CNT	18.624	18.624	7.681	1.610	2.42	11.57	—	1.409	0.209

[a] μmol/mg, the quantities of charge and gas have been normalized to the total mass of the respective cathodes. D: discharge; R: recharge; C: consumption of gas during discharge; E: evolution of gas during recharge.

chemical cycle, the amount of O_2 consumed during discharge is equal to that of O_2 evolved in the subsequent recharge, and O_2 is the only gaseous species involved in the discharge/recharge cycle. To compare the DEMS results of different Li-O_2 cells in a straightforward way (experimental details can be found in Supporting Information), we cycled the cells with a fixed capacity of 500 mAh/g (normalized to the total mass of the cathode) at a constant current of 0.6 mA (absolute current) for both discharge and recharge half cycle and simultaneously measured the rate of O_2 consumption/evolution during discharge/recharge. By integrating the area under the curves of the O_2 consumption rate and comparing with the amount of charge passed during discharge (Supporting Information Figure S5a, Figure 3a,b for the pristine CNT, Ru-CNT, and Pd-CNT cathodes, respectively), we obtained the ratios of the number of electrons to per O_2 molecule (e^-/O_2) for the discharge reactions on the pristine and catalyzed CNT cathodes, see Table 1. For pristine and Ru-CNT cathode, values of 2.02 and 2.08 e^-/O_2 have been obtained, which are close to the 2.00 e^-/O_2 for the desired O_2 reduction to Li_2O_2, while a much deviated value of 2.42 e^-/O_2 was obtained for Pd-CNT cathode, suggesting an elevated extent of the parasitic reactions during the discharge process. No CO_2 evolution was observed in the course of discharge for the above three cathodes.

To obtain more information on the discharge products of the pristine and catalyzed Li-O_2 cells, Fourier transform infrared spectroscopy (FTIR) has also been used to analyze the respective cathodes after discharging to a fixed capacity of 1000 mAh/g_{carbon} at a current density of 100 mA/g_{carbon}, see Figure 4a. For comparison, a pristine CNT electrode has also been discharged under the same conditions and then analyzed. A band at ~500 cm^{-1} for each of the cathodes indicates the precipitation of Li_2O_2. The bands at ~870, 1500, and 1600 cm^{-1} show the presence of Li_2CO_3 and HCO_2Li, two typical byproducts that have been widely identified at the end of discharge of Li-O_2 cells containing ether-based electrolytes.[9,13,54] A subsequent SEM study revealed the formation of disk-like solids (Figure 4b,c), a morphology of Li_2O_2

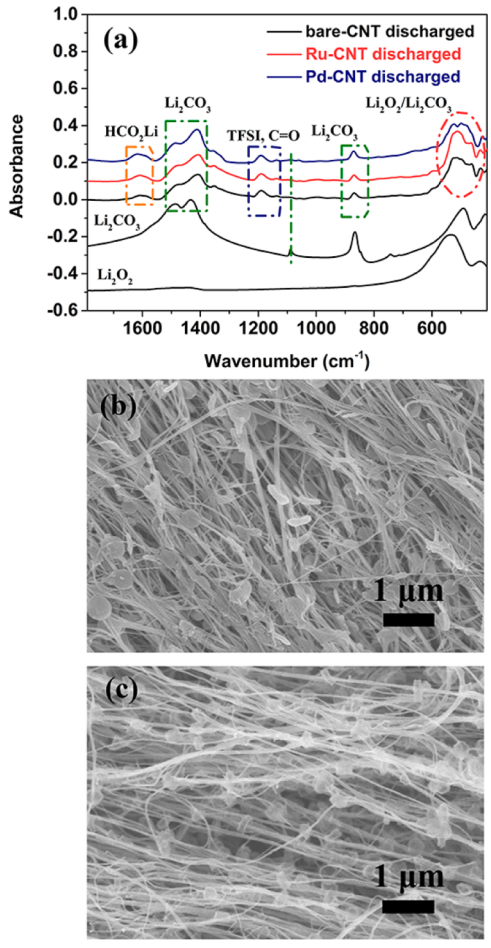

Figure 4. (a) FTIR spectra of Ru/Pd-CNT and pristine CNT cathodes at the end of discharge, and SEM images of (b) Ru-CNT and (c) Pd-CNT cathodes at the end of discharge. The FTIR spectra in (a) are vertically shifted for clarity.

DOI: 10.1021/acs.nanolett.5b03510
Nano Lett. 2015, 15, 8084−8090

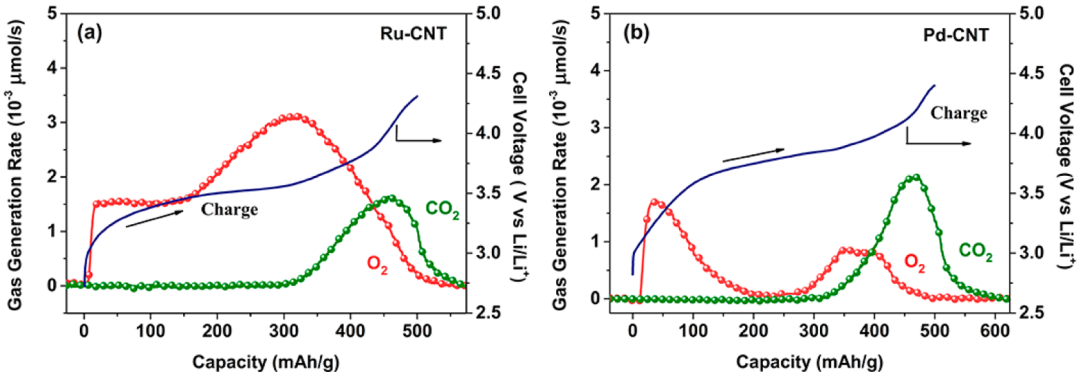

Figure 5. DEMS results of O_2 and CO_2 evolution during the charging process of Li-O_2 cells based on (a) Ru-CNT and (b) Pd-CNT cathodes.

produced in Li-O_2 batteries under low rate/overpotential conditions.[60] However, the Li_2CO_3 and HCO_2Li formed within the CNT cathodes can hardly manifest themselves in SEM (Figure 4b,c) or XRD (Supporting Information Figure S6) studies, probably due to their poorly crystalline natures, owing to the increased coverage of Li_2O_2 particles on CNT fibril with continued discharge to higher capacity.[61] Besides their footprints observed with FTIR, the formation of Li_2O_2 and Li_2CO_3 at the end of discharge is also confirmed by an analysis with Raman spectroscopy (Supporting Information Figure S7a,b). The appearance of Li_2CO_3 has been proposed to be due to the chemical reaction between Li_2O_2 and carbon-based electrode[61] or ether-based electrolyte catalyzed by Ru and Pd catalysts. These spectroscopic results provide direct evidence that parasitic reaction does occur during discharge of the Li-O_2 cells, even for those based on pristine CNT cathodes with a value of e^-/O_2 close to 2.0. The existence of parasitic reactions inevitably impairs the cells' reversibility, because all of the byproducts are carbon-based and must derive from the decomposition of either the electrolyte or CNT support, or both.

Turning our attention to the recharge process, the rate of O_2 evolution upon oxidation of the Li_2O_2 formed in the preceding discharge was also quantified with DEMS. Instead of exhibiting a stable evolution rate, two separate O_2 generation peaks, appearing at early and later stage of recharge, respectively, were observed (Figure 5a,b and Supporting Information Figure S5b). This phenomenon has been observed before.[40,62] This observed O_2 generation in DEMS experiments can be attributed to the decomposition of Li_2O_2 rather than other byproducts.[63] The release of O_2 at the initial stage of charging with low overpotentials may imply that Ru/Pd particles could function as electro-catalysts. To shed light on OER process, additional FTIR studies have been carried out for the cathodes charged to different stages (Supporting Information Figures S8−10), which provide direct evidence that at the early stage of charging, only Li_2O_2 has been oxidized instead of other byproducts, by comparing the FTIR intensity of Li_2O_2 at 530 cm^{-1} with that of Li_2CO_3 at 867 cm^{-1} and HCO_2Li at 1608 cm^{-1} (Supporting Information Tables S1−3). Moreover, the quantity of the released O_2, calculated by integrating of the area under the curves of O_2 evolution rate, was compared with the charge passed during the recharge process. Values of 3.08, 3.14, and 11.57 e^-/O_2 were obtained for the pristine and Ru- and Pd-CNT cathodes, respectively, and all these values deviated significantly from the ideal 2.00 e^-/O_2 for the desired Li_2O_2 oxidation to O_2, particularly for the case of Pd-CNT electrode. By comparing the O_2 consumption and evolution during a full discharge/charge cycle, O_2 recovery efficiencies have been quantified to be 0.654, 0.662, and 0.209 for the pristine and Ru- and Pd-CNT cathodes, respectively, see Table 1 for details.

A e^-/O_2 much >2 upon recharge, unbalanced O_2 consumption and evolution, and the O_2 recovery efficiency much <1, altogether provides strong evidence that severe parasitic reactions occur in the discharge and/or recharge process. The existence of parasitic reactions is further evidenced by the concomitant CO_2 evolution at the later stage of recharge in all of the three cathodes (Figure 5a,b and Supporting Information Figure S5b). Actually, the appearance of gaseous CO_2 during recharge is an indicator that the Li-O_2 cells are not ideally reversible, and the amount of CO_2 generated (Table 1) directly reveals the extent of undesired side reactions, which has been suggested to originate from the decomposition of carbon cathode or electrolyte.[9,54,64] Clearly, the presence of noble metal catalysts does not necessarily improve the reversibility of the aprotic Li-O_2 batteries, and particularly in the case of nano-Pd catalyst which results in a drastically decreased O_2 recovery efficiency and the generation of considerable amount of CO_2 during recharge. For Ru-catalyzed Li-O_2 cells, the slightly increased O_2 recovery efficiency and the decreased over-potentials (particularly for recharge) suggest the possibility of electro-catalysis, at least at the early stage of recharge. The small amount of CO_2 evolved in the pristine cathodes during recharging may be due to the incomplete removal of side products such as Li_2CO_3. However, more studies are needed before a final conclusion can be made, by using more stable combinations of electrode materials and electrolytes, so as to lower the extent of the parasitic reactions and reveal the intrinsic activity of Ru toward the O_2 reactions. In view of our results, the function of a wide spectrum of noble metal catalysts reported in the literatures[41−45] that have been claimed to catalyze the oxidation of Li_2O_2 should therefore be further examined. Quantitative measurements of O_2 reactions in Li-O_2 cells, such as DEMS exemplify here for the O_2 consumption/evolution and the reversibility, are essential in the course of pursuing truly rechargeable Li-O_2 batteries.

Conclusions. In summary, noble metal (Ru and Pd)-catalyzed CNT fabrics, prepared by magnetron sputtering, have been used as the O_2 cathodes for the aprotic Li-O_2 batteries. Although these noble metal-CNT composite cathodes exhibited excellent electrochemical performances in terms of round-trip efficiency and cycle life, *in situ* DEMS studies coupled with *ex situ* spectroscopic analyses, however, revealed that these catalyzed Li-O_2 batteries did not work according to

DOI: 10.1021/acs.nanolett.5b03510
Nano Lett. 2015, 15, 8084−8090

the desired Li-O_2 reactions, demonstrating a reversibility even poorer than their counterpart using pristine CNT cathodes. The results reported here provide new insights into the O_2 electrochemistry in the aprotic Li-O_2 batteries containing noble metal catalysts and exemplified the importance of a quantitative assay of the O_2 electrochemistry in the course of pursuing truly rechargeable Li-O_2 batteries.

■ ASSOCIATED CONTENT

Supporting Information

The Supporting Information is available free of charge on the ACS Publications website at DOI: 10.1021/acs.nanolett.5b03510.

Experimental details; the fabrication procedure and photograph of samples of Ru/Pd-CNT fabric electrodes; EDX, XRD, and TGA data for Ru/Pd-CNT electrodes; cycle performances and DEMS results of the pristine CNT-based Li-O_2 cell; the XRD patterns and Raman data of Ru/Pd-CNT cathode before and after discharge; additional FTIR spectra of cathodes being recharged to different stages (PDF)

■ AUTHOR INFORMATION

Corresponding Authors

*E-mail: wuyang.thu@gmail.com.
*E-mail: zqpeng@ciac.ac.cn.

Notes

The authors declare no competing financial interest.

■ ACKNOWLEDGMENTS

Z.P. is indebted to the National Science Foundation of China (grant no. 21575135), the "Strategic Priority Research Program" of the Chinese Academy of Sciences (grant no. XDA09010401), the "Recruitment Program of Global Youth Experts" of China. Y.W. thanks the support from the National Basic research program of China (grant. no. 2012CB932301), the National Science Foundation of China (grant no. 51472141, 51472142), and Chinese Postdoctoral Science Foundation (grant no. 2012M520261 and 2014T70076). Y.X. is indebted to the Science and Technology Development Program of the Jilin Province (grant no. 20150623002TC).

■ REFERENCES

(1) Abraham, K. M.; Jiang, Z. *J. Electrochem. Soc.* **1996**, *143*, 1−5.
(2) Armand, M.; Tarascon, J.-M. *Nature* **2008**, *451*, 652−657.
(3) Girishkumar, G.; McCloskey, B. D.; Luntz, A. C.; Swanson, S.; Wilcke, W. *J. Phys. Chem. Lett.* **2010**, *1*, 2193−2203.
(4) Bruce, P. G.; Freunberger, S. A.; Hardwick, L. J.; Tarascon, J.-M. *Nat. Mater.* **2012**, *11*, 19−29.
(5) Lu, J.; Li, L.; Park, J.-B.; Sun, Y.-K.; Wu, F.; Amine, K. *Chem. Rev.* **2014**, *114*, 5611−5640.
(6) Li, F.; Zhang, T.; Zhou, H. *Energy Environ. Sci.* **2013**, *6*, 1125−1141.
(7) Lu, Y.-C.; Gallant, B. M.; Kwabi, D. G.; Harding, J. R.; Mitchell, R. R.; Whittingham, M. S.; Shao-Horn, Y. *Energy Environ. Sci.* **2013**, *6*, 750−768.
(8) Luntz, A. C.; McCloskey, B. D. *Chem. Rev.* **2014**, *114*, 11721−11750.
(9) Peng, Z.; Freunberger, S. A.; Chen, Y.; Bruce, P. G. *Science* **2012**, *337*, 563−566.
(10) Jung, H.-G.; Hassoun, J.; Park, J.-B.; Sun, Y.-K.; Scrosati, B. *Nat. Chem.* **2012**, *4*, 579−585.
(11) Peng, Z.; Freunberger, S. A.; Hardwick, L. J.; Chen, Y.; Giordani, V.; Bardé, F.; Novák, P.; Graham, D.; Tarascon, J.-M.; Bruce, P. G. *Angew. Chem.* **2011**, *123*, 6475−6479.
(12) Chen, Y.; Freunberger, S. A.; Peng, Z.; Bardé, F.; Bruce, P. G. *J. Am. Chem. Soc.* **2012**, *134*, 7952−7957.
(13) Freunberger, S. A.; Chen, Y.; Drewett, N. E.; Hardwick, L. J.; Bardé, F.; Bruce, P. G. *Angew. Chem., Int. Ed.* **2011**, *50*, 8609−8631.
(14) Lu, Y.-C.; Xu, Z.; Gasteiger, H. A.; Chen, S.; Hamad-Schifferli, K.; Shao-Horn, Y. *J. Am. Chem. Soc.* **2010**, *132*, 12170−12171.
(15) Lu, Y.-C.; Gasteiger, H. A.; Shao-Horn, Y. *J. Am. Chem. Soc.* **2011**, *133*, 19048−19051.
(16) Zhu, D.; Zhang, L.; Song, M.; Wang, X.; Chen, Y. *Chem. Commun.* **2013**, *49*, 9573−9575.
(17) Harding, J. R.; Lu, Y.-C.; Tsukada, Y.; Shao-Horn, Y. *Phys. Chem. Chem. Phys.* **2012**, *14*, 10540−10546.
(18) Lu, Y.-C.; Gasteiger, H. A.; Parent, M. C.; Chiloyan, V.; Shao-Horn, Y. *Electrochem. Solid-State Lett.* **2010**, *13*, A69−A72.
(19) Oh, S. H.; Black, R.; Pomerantseva, E.; Lee, J.-H.; Nazar, L. F. *Nat. Chem.* **2012**, *4*, 1004−1010.
(20) Black, R.; Lee, J.-H.; Adams, B.; Mims, C. A.; Nazar, L. F. *Angew. Chem.* **2013**, *125*, 410−414.
(21) Oh, S. H.; Nazar, L. F. *Adv. Energy Mater.* **2012**, *2*, 903−910.
(22) Débart, A.; Paterson, A. J.; Bao, J.; Bruce, P. G. *Angew. Chem.* **2008**, *120*, 4597−4600.
(23) Ma, S.; Sun, L.; Cong, L.; Gao, X.; Yao, C.; Guo, X.; Tai, L.; Mei, P.; Zeng, Y.; Xie, H.; Wang, R. *J. Phys. Chem. C* **2013**, *117*, 25890−25897.
(24) Zhang, L.; Zhang, S.; Zhang, K.; Xu, G.; He, X.; Dong, S.; Liu, Z.; Huang, C.; Gu, L.; Cui, G. *Chem. Commun.* **2013**, *49*, 3540−3542.
(25) Xu, J.-J.; Xu, D.; Wang, Z.-L.; Wang, H.-G.; Zhang, L.-L.; Zhang, X.-B. *Angew. Chem., Int. Ed.* **2013**, *52*, 3887−3890.
(26) Zhao, Y.; Xu, L.; Mai, L.; Han, C.; An, Q.; Xu, X.; Liu, X.; Zhang, Q. *Proc. Natl. Acad. Sci. U. S. A.* **2012**, *109*, 19569−19574.
(27) Chen, Y.; Freunberger, S. A.; Peng, Z.; Fontaine, O.; Bruce, P. G. *Nat. Chem.* **2013**, *5*, 489−494.
(28) Lacey, M. L.; Frith, J. T.; Owen, J. R. *Electrochem. Commun.* **2013**, *26*, 74−76.
(29) Sun, D.; Shen, Y.; Zhang, W.; Yu, L.; Yi, Z.; Yin, W.; Wang, D.; Huang, Y.; Wang, J.; Wang, D.; Goodenough, J. B. *J. Am. Chem. Soc.* **2014**, *136*, 8941−8946.
(30) Mitchell, R. R.; Gallant, B. M.; Thompson, C. V.; Shao-Horn, Y. *Energy Environ. Sci.* **2011**, *4*, 2952−2958.
(31) Wu, G.; Mack, N. H.; Gao, W.; Ma, S.; Zhong, R.; Han, J.; Baldwin, J. K.; Zelenay, P. *ACS Nano* **2012**, *6*, 9764−9776.
(32) Yoo, E.; Zhou, H. *ACS Nano* **2011**, *5*, 3020−3026.
(33) Xiao, J.; Mei, D.; Li, X.; Xu, W.; Wang, D.; Graff, G. L.; Bennett, W. D.; Nie, Z.; Saraf, L. V.; Aksay, I. A.; Liu, J.; Zhang, J.-G. *Nano Lett.* **2011**, *11*, 5071−5078.
(34) Wang, Z.-L.; Xu, D.; Xu, J.-J.; Zhang, L.-L.; Zhang, X.-B *Adv. Funct. Mater.* **2012**, *22*, 3699−3705.
(35) Zhang, W.; Zhu, J.; Ang, H.; Zeng, Y.; Xiao, N.; Gao, Y.; Liu, W.; Hng, H.; Yan, Q. *Nanoscale* **2013**, *5*, 9651−9658.
(36) Lim, H.-D.; Park, K.-Y.; Song, H.; Jang, E. Y.; Gwon, H.; Kim, J.; Kim, Y. H.; Lima, M. D.; Ovalle-Robles, R.; Lepró, X.; Baughman, R. H.; Kang, K. *Adv. Mater.* **2013**, *25*, 1348−1352.
(37) Thotiyl, M. M. O.; Freunberger, S. A.; Peng, Z.; Chen, Y.; Liu, Z.; Bruce, P. G. *Nat. Mater.* **2013**, *12*, 1050−1056.
(38) Li, F.; Tang, D.-M.; Chen, Y.; Golberg, D.; Kitaura, H.; Zhang, T.; Yamada, A.; Zhou, H. *Nano Lett.* **2013**, *13*, 4702−4707.
(39) Li, F.; Tang, D.-M.; Jian, Z.; Liu, D.; Golberg, D.; Yamada, A.; Zhou, H. *Adv. Mater.* **2014**, *26*, 4659−4664.
(40) Xie, J.; Yao, X.; Madden, I. P.; Jiang, D.-E.; Chou, L.-Y.; Tsung, C.-K.; Wang, D. *J. Am. Chem. Soc.* **2014**, *136*, 8903−8906.
(41) Jung, H.-G.; Jesong, Y. S.; Park, J.-B.; Sun, Y.-K.; Scrosati, B.; Lee, Y. J. *ACS Nano* **2013**, *7*, 3532−3539.
(42) Lim, H.-D.; Song, H.; Gwon, H.; Park, K.-Y.; Kim, J.; Bae, Y.; Kim, H.; Jung, S.-K.; Kim, T.; Kim, Y. H.; Lepró, X.; Ovalle-Robles, R.; Baughman, R. H.; Kang, K. *Energy Environ. Sci.* **2013**, *6*, 3570−3575.

DOI: 10.1021/acs.nanolett.5b03510
Nano Lett. 2015, 15, 8084−8090

(43) Lu, J.; Lei, Y.; Lau, K. C.; Luo, X.; Du, P.; Wen, J.; Assary, R. S.; Das, U.; Miller, D. J.; Elam, J. W.; Albishri, H. M.; El-Hady, D. A.; Sun, Y.-K.; Curtiss, L. A.; Amine, K. *Nat. Commun.* **2013**, *4*, 2383.
(44) Zeng, X.; You, C.; Leng, L.; Dang, D.; Qiao, X.; Li, X.; Li, Y.; Liao, S.; Adizic, R. R. *J. Mater. Chem. A* **2015**, *3*, 11224−11231.
(45) Shen, Y.; Sun, D.; Yu, L.; Zhang, W.; Shang, Y.; Tang, H.; Wu, J.; Cao, A.; Huang, Y. *Carbon* **2013**, *62*, 288−295.
(46) Wang, J.-T.; Wasmus, S.; Savinell, R. F. *J. Electrochem. Soc.* **1996**, *143*, 1233−1239.
(47) Seiler, T.; Savinova, E. R.; Friedrich, K. A.; Stimming, U. *Electrochim. Acta* **2004**, *49*, 3927−3936.
(48) Niether, C.; Rau, M. S.; Cremers, C.; Jones, D. J.; Pinkwart, K.; Tübke. *J. Electroanal. Chem.* **2015**, *747*, 97−103.
(49) Imhof, R.; Novák, P. *J. Electrochem. Soc.* **1999**, *146*, 1702−1706.
(50) Armstrong, A. R.; Holzapfel, M.; Novák, P.; Johnson, C. S.; Kang, S.-H.; Thackeray, M. M.; Bruce, P. G. *J. Am. Chem. Soc.* **2006**, *128*, 8694−8698.
(51) Wang, H.; Rus, E.; Sakuraba, T.; Kikuchi, J.; Kiya, Y.; Abruña, H. D. *Anal. Chem.* **2014**, *86*, 6197−6201.
(52) McCloskey, B. D.; Scheffler, R.; Speidel, A.; Bethune, D. S.; Shelby, R. M.; Luntz, A. C. *J. Am. Chem. Soc.* **2011**, *133*, 18038−18041.
(53) McCloskey, B. D.; Bethune, D. S.; Shelby, R. M.; Girishkumar, G.; Luntz, A. C. *J. Phys. Chem. Lett.* **2011**, *2*, 1161−1166.
(54) Gowda, S. R.; Brunet, A.; Wallraff, G. M.; McCloskey, B. D. *J. Phys. Chem. Lett.* **2013**, *4*, 276−279.
(55) Meini, S.; Solchenbach, S.; Piana, M.; Gasteiger, H. A. *J. Electrochem. Soc.* **2014**, *161*, A1306−A1314.
(56) Wu, Y.; Wei, Y.; Wang, J.; Jiang, K.; Fan, S. *Nano Lett.* **2013**, *13*, 818−823.
(57) Jiang, K.; Li, Q.; Fan, S. *Nature* **2002**, *419*, 801−801.
(58) Jiang, K.; Wang, J.; Li, Q.; Liu, L.; Li, C.; Fan, S. *Adv. Mater.* **2011**, *23*, 1154−1161.
(59) Dathar, G. K. P.; Shelton, W. A.; Xu, Y. *J. Phys. Chem. Lett.* **2012**, *3*, 891−895.
(60) Adams, B. D.; Radtke, C.; Black, R.; Trudeau, M. L.; Zaghib, K.; Nazar, L. F. *Energy Environ. Sci.* **2013**, *6*, 1772−1778.
(61) Gallant, B. M.; Mitchell, R. R.; Kwabi, D. G.; Zhou, J.; Zuin, L.; Thompson, C. V.; Shao-Horn, Y. *J. Phys. Chem. C* **2012**, *116*, 20800−20805.
(62) Kundu, D.; Black, R.; Berg, E. J.; Nazar, L. F. *Energy Environ. Sci.* **2015**, *8*, 1292−1298.
(63) Meini, S.; Tsiouvaras, N.; Schwenke, K. U.; Piana, M.; Beyer, H.; Lange, L.; Gasteiger, H. A. *Phys. Chem. Chem. Phys.* **2013**, *15*, 11478−11493.
(64) Thotiyl, M. M. O.; Freunberger, S. A.; Peng, Z.; Bruce, P. G. *J. Am. Chem. Soc.* **2013**, *135*, 494−500.

DOI: 10.1021/acs.nanolett.5b03510
Nano Lett. 2015, 15, 8084−8090